

Carbon-Supported Pt-RuCo Nanoparticles With Low-Noble-Metal Content and Superior Catalysis for Ethanol Oxidization

Hao Li¹, Deli Kang², Hui Wang², Rongfang Wang^{2,*}

¹ Department of Chemical Engineering, Huizhou University, Huizhou, Guangdong 516007, China

² Key Laboratory of Eco-Environment-Related Polymer Materials, Ministry of Education of China, Key Laboratory of Gansu Polymer Materials, College of Chemistry and Chemical Engineering, Northwest Normal University, Lanzhou 730070, China

*E-mail: wrf38745779@126.com

Received: 14 February 2010 / Accepted: 15 March 2010 / Published: 1 April 2011

To improve the catalytic activity and lower the noble-metal loading of electrocatalysts for ethanol electrooxidation, a carbon-supported Pt-RuCo catalyst (atomic ratio of Pt : Ru : Co = 1 : 2.5 : 5.2) is prepared by a two-step route. The as-prepared catalyst is characterized by means of X-ray diffraction (XRD), transmission electron microscopy (TEM), as well as cyclic voltammetry technique. The Pt-RuCo/C sample is found to possess good electrocatalytic performance, long-term durability and high CO-tolerance, which should have potential application in electrocatalyst of direct ethanol fuel cell.

Keywords: Electrocatalyst, ethanol oxidization, nanoparticles, fuel cell

1. INTRODUCTION

In the past decade, direct ethanol fuel cell (DEFC) has received much attention due to its potential applications in portable and mobile power sources [1-5]. However, there are still several obstacles, such as insufficient activities and high cost of anode catalysts, hindering the commercial application of DEFC [6-9]. Pt is the most active catalytic material for ethanol oxidation, however, it is vulnerable because it is easily poisoned by strongly adsorbed species like CO, which will result in significant decrease in electrocatalytic activities [10]. Furthermore, Pt is very costly owing to its limited resources. Hence, one of the objectives in the ongoing work on DEFC is to develop catalysts with both low Pt loading and high catalytic activities.

It has been well demonstrated that the electrocatalytic activity of Pt catalyst to alcohol oxidation can be improved by the addition of other metals to Pt [11-15]. For example, Pt-Ru-Co tri-

metallic catalyst is reported to be a good candidate for the substitution of Pt catalyst. Recently, Huang et al. have reported the preparation of nanosized Pt-Ru-Co (at molar ratio of 6:3:1) particles dispersed on multi-wall carbon nanotubes by an ultrasonic-assisted chemical reduction [16]. Moreno et al. have also fabricated Pt-Ru-Co (at molar ratio of 60:30:10) nanoparticles by a combustion route [17]. Though both groups have demonstrated the high electrocatalytic activities of their catalysts, the relatively high content of noble metal in the catalysts makes them less attractive from the viewpoint of the cost of catalysts. Obviously, Pt-Ru-Co catalysts with both low content of noble metal and high electrocatalytic activity are still highly desirable.

In this study, a carbon-supported Pt modified RuCo (denoted as Pt-RuCo/C) catalyst with low Pt content (atomic ratio of Pt : Ru : Co = 1 : 2.5 : 5.2) is prepared by a facile two-step route. The as-prepared catalyst is characterized by means of X-ray diffraction (XRD) and transmission electron microscopy (TEM). The electrocatalytic activity is also tested for ethanol electrooxidation by cyclic voltammetry technique. The results indicate that the Pt-RuCo/C has a better catalytic performance than Pt/C and PtRu/C.

2. EXPERIMENTAL

The Pt-RuCo/C catalyst was prepared by a two-step route in an ethylene glycol (EG) solution. Ruthenium chloride (RuCl_3), cobalt nitrate hexahydrate ($\text{Co}(\text{NO}_3)_2 \cdot 6\text{H}_2\text{O}$) and sodium formate ($\text{HCOONa} \cdot 2\text{H}_2\text{O}$) was dissolved in ethylene glycol (EG) and stirred for 0.5 h. Carbon black Vulcan XC-72 was then added to the mixture (total metal loading: 40%, and Ru : Co = 1 : 3 in atomic ratio) under stirred conditions. The pH of the system was adjusted to about 10 by the dropwise addition of a 5 wt% KOH/EG solution with vigorous stirring. The mixture was then placed into a flask and stirred at 180 °C for 8 h. After reaction, the powders were collected by filtration, then washed with deionized water, and finally dried in a vacuum oven at 60 °C for 12 h. For comparison, Pt/C (20 wt% Pt) and PtRu/C (20 wt% Pt and 10 wt% Ru) catalysts were also prepared by the same procedure except that H_2PtCl_6 and $\text{H}_2\text{PtCl}_6/\text{RuCl}_3$ instead of $\text{H}_2\text{PtCl}_6/\text{Co}(\text{NO}_3)_2 \cdot 6\text{H}_2\text{O}$ was used as the precursors, respectively.

To obtain Pt-RuCo/C catalyst, the collected RuCo/C powders were added to a flask containing EG solution of chloroplatinic acid (H_2PtCl_6) (Pt : RuCo = 1 : 4 in weight ratio) and sodium citrate ($\text{C}_6\text{H}_5\text{O}_7 \cdot 2\text{H}_2\text{O}$) at 160 °C for 13 h. After reaction, the mixture was acidified by adding nitric acid solution to achieve a pH of about 4, then filtered and washed with deionized water, finally dried in vacuum oven at 60 °C for 12 h.

The catalysts were structurally characterized by recording their XRD patterns on a D/MAX-III A (Rigaku Corporation, Japan) X-ray diffractometer with Cu $K\alpha$ radiation ($\lambda = 1.5406 \text{ \AA}$). The TEM measurements were carried out on a Tecnai G220S-TWIN (FEI Company) with the acceleration voltage of 200 kV. The average chemical composition of Pt-RuCo/C catalyst was determined using an IRIS advantage inductively coupled plasma atomic emission spectroscopy (ICP-AES) system (Thermo, America).

The electrochemical measurements of catalysts were performed using an electrochemical workstation (RST3000). A three-electrode electrochemical cell was used for the measurements. The counter and reference electrodes were a platinum wire and an Ag/AgCl (3 M) electrode, respectively. The working electrode was a glassy carbon disk (5mm in diameter). The thin-film electrode was prepared as follows: 5 mg catalyst was dispersed ultrasonically in 1mL Nafion/ethanol (0.25 % Nafion) for 15 min. About 8 μ L of the dispersion was transferred onto the glassy carbon disk using a pipet, and then dried in the air.

3. RESULTS AND DISCUSSION

The chemical composition of the Pt-RuCo/C catalyst was determined by ICP-AES analysis, which is about Pt:Ru:Co = 1:2.5:5.2 (atomic ratio). This is a consequence of the stoichiometry of the replacement reaction which exchange the Pt atoms with Co atoms, considering the nominal atomic ratio of Pt, Ru and Co in the starting precursor.

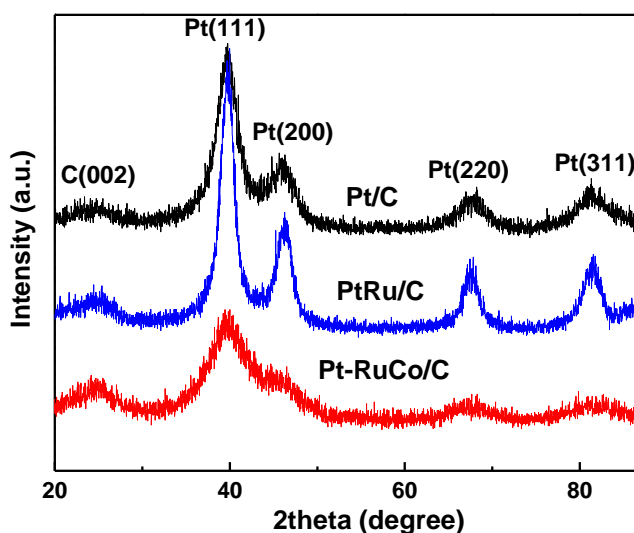


Figure 1. The XRD patterns of the Pt/C, PtRu/C and Pt-RuCo/C catalysts.

The XRD patterns of the as-prepared Pt/C, PtRu/C and Pt-RuCo/C catalysts are shown in Fig. 1. The peak located at $2\theta = 24.8^\circ$ in all the XRD patterns is associated with the carbon support. The other peaks at 2θ value of ca. 40° , 47° , 68° , 81° can be assigned to diffraction from the (111), (200), (220) and (311) planes of face center cubic (fcc) crystalline Pt or Pt-based alloy (PtRu/C or Pt-RuCo/C), respectively. It can be clearly observed that the intensities of the characteristic peak of Pt-RuCo/C are pronouncedly lower than those of Pt/C and PtRu/C, implying that Pt-RuCo has smaller particle size compared with Pt and PtRu. According to Scherer equation [18], the average particle size of Pt/C, PtRu/C and Pt-RuCo calculated from the width of (220) diffraction peak is about 3.4 nm, 4.4

nm and 2.8 nm, respectively. Note that the mean particle size of the as-prepared Pt-RuCo catalysts is close to that of Pt_{0.6}Ru_{0.3}Co_{0.1} (2.61 nm [16]) prepared by ultrasonic-assisted chemical reduction, while it is significantly smaller than that of Pt_{0.6}Ru_{0.3}Co_{0.1} (19 nm [17]) prepared via urea combustion.

The XRD-determined surface areas (SXR) are estimated using an equation $S = 6000/rd$ [17], where r is the particle size in nm, obtained from the XRD data, and d is the density of the metallic catalyst. The density values are 21.45, 12.20 and 8.90 g cm⁻³ for Pt, Pd and Co, respectively. Accordingly, the SXR are calculated to be 82.3 m² g⁻¹ for Pt/C, 74.1 m² g⁻¹ for PtRu/C and 155.4 m² g⁻¹ for Pt-RuCo/C, respectively.

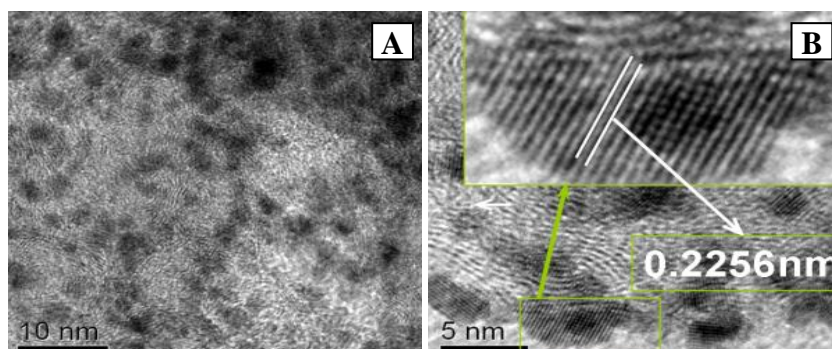


Figure 2. TEM image (A) and high resolution TEM image (B) of Pt-RuCo/C catalysts.

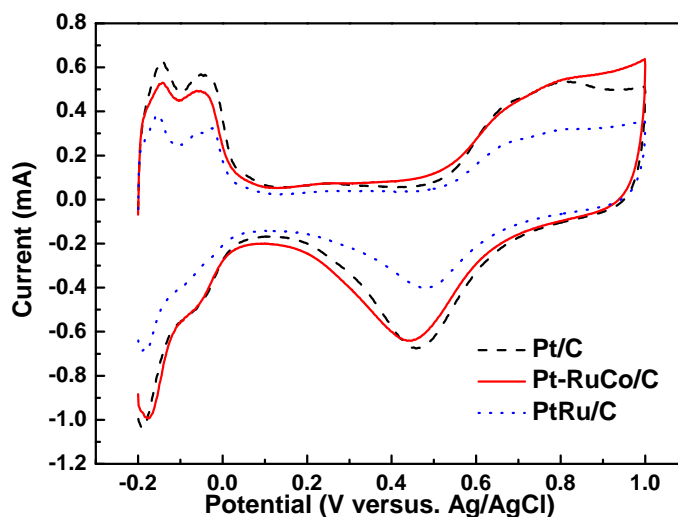


Figure 3. Cyclic voltammograms of the Pt-RuCo/C, PtRu/C and Pt/C catalysts in 0.5 M H₂SO₄ solution under N₂ atmosphere; scan rate: 50 mV s⁻¹, room temperature.

The Pt-RuCo/C catalyst is examined by TEM and the results are presented in Fig. 2. It is observed that the Pt-RuCo nanoparticles with uniform size distribution are well dispersed on the carbon support. The Pt-RuCo particle sizes range from 2.5 to 4.2 nm with a mean value of ca. 3.0 nm, which is in good agreement with the result from XRD data. The high resolution TEM image shows the

lattice distance in the Pt-RuCo catalysts is 0.2256 nm, corresponding to the lattice spacing of the (111) plane of the face-centered cubic Pt crystal (0.23 nm). Considering that Pt is produced by the reduction of H_2PtCl_6 with Co on the surface of RuCo and the interaction between the metals is stronger than that between metal and carbon, it is likely that Pt covers the RuCo particles [19].

The electrocatalytic activity of the catalysts is characterized by cyclic voltammetry (CV) technique. Fig. 3 shows the CV curves of the Pt-RuCo/C, PtRu/C and Pt/C measured in 0.5 M H_2SO_4 solution under N_2 atmosphere at a scan rate of 50 mV s^{-1} . There are three distinct potential regions in the voltammograms: the hydrogen adsorption/desorption region (from 0 to 0.3 V versus RHE), the double-layer region (from 0.3 to 0.7 V), and the surface oxide (OH_{ads}) formation/stripping region (>0.7 V). The electrochemical surface area of Pt particles is a important concern and the large electrochemical surface area is always desirable in view of the fact that the catalytic reactions often occur on the surface of the catalyst. The real surface of Pt-based catalysts could be estimated from the integrated charge of the hydrogen absorption region of the CV. The electrochemical active surface areas of different catalysts was calculated according to the following formula assuming a correlation value of 0.21 mC cm^{-2} and Pt loading [19, 20]

$$A_{\text{EL}}(\text{m}^2 \text{ g}^{-1}_{\text{Pt}}) = Q_{\text{H}} / (0.21 \times 10^{-3} \text{ C} \times g_{\text{Pt}}) \quad (1)$$

where A_{EL} is the Pt surface obtained electrochemically, Q_{H} is the amount of charge exchanged during the electroadsorption of hydrogen atoms on Pt and g_{Pt} is the Pt loading on the electrode. The calculated A_{EL} are $233.33 \text{ m}^2 \text{ g}^{-1}_{\text{Pt}}$ for Pt-RuCo/C, $56.50 \text{ m}^2 \text{ g}^{-1}_{\text{Pt}}$ for PtRu/C and $66.67 \text{ m}^2 \text{ g}^{-1}_{\text{Pt}}$ for Pt/C, respectively, indicating that the Pt-RuCo/C has the largest A_{EL} .

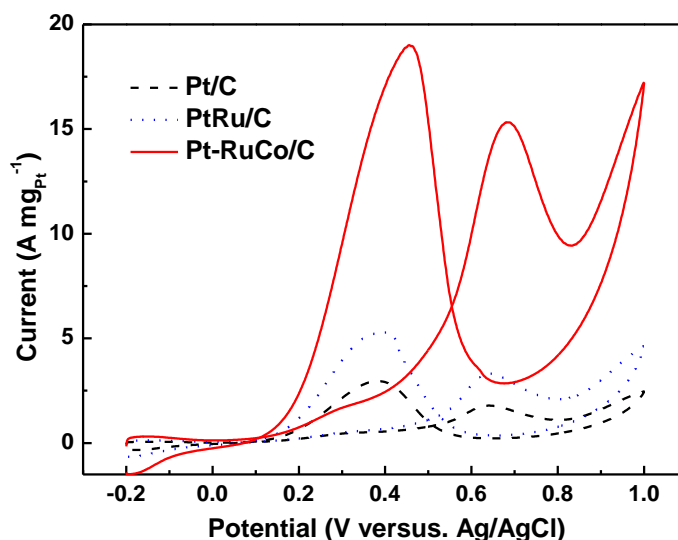


Figure 4. Cyclic voltammograms of ethanol electrooxidation in an N_2 -saturated solution of 0.5 mol L^{-1} $\text{CH}_3\text{CH}_2\text{OH}$ and 0.5 mol L^{-1} H_2SO_4 at room temperature on the Pt-RuCo/C, Pt/C and PtRu/C catalysts. Scan rate: 50 mV s^{-1} , rotation speed: 300 rpm (the data are derived from the glassy carbon based electrode measurements).

Fig. 4. displays the cyclic voltammograms of ethanol electrooxidation on the Pt-RuCo/C, Pt/C and PtRu/C catalysts in an N_2 -saturated solution of $0.5 \text{ mol L}^{-1} \text{ CH}_3\text{CH}_2\text{OH}$ and $0.5 \text{ mol L}^{-1} \text{ H}_2\text{SO}_4$ at room temperature. Obviously, the Pt-RuCo/C exhibits superior catalytic activity to PtRu/C and Pt/C, that is, lower onset potential and higher oxidation current density. During positive potential scanning, the mass activity value of Pt-RuCo/C is $15.35 \text{ A mg}_{\text{Pt}}^{-1}$, which is 4.55 times and 8.58 times as large as that of PtRu/C and Pt/C, respectively. During its reverse scanning, the peak current density on the Pt-RuCo/C catalyst is $19.00 \text{ A mg}_{\text{Pt}}^{-1}$, which is 2.57 times and 5.35 times higher than that of PtRu/C and Pt/C, respectively. Compared to the PtRu/C, such an excellent catalytic activity of the Pt-RuCo/C is mainly due to the increased active surface area.

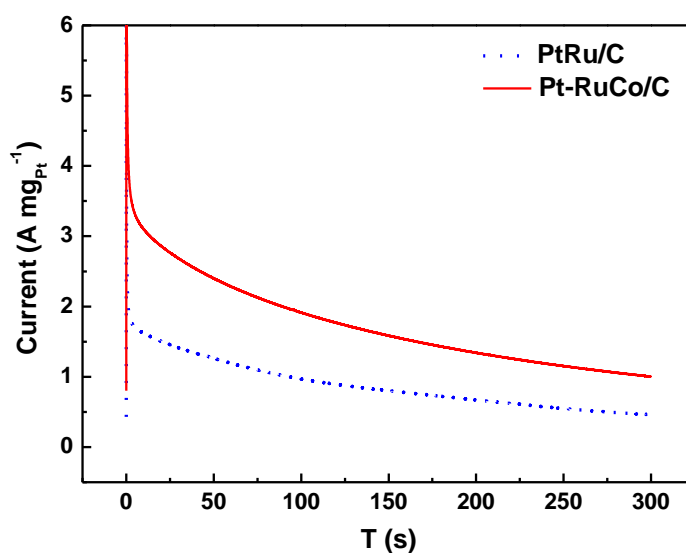


Figure 5. The chronoamperometric curves in an N_2 -saturated solution of $0.5 \text{ M CH}_3\text{CH}_2\text{OH}$ in $0.5 \text{ M H}_2\text{SO}_4$ solution on the Pt-RuCo/C and PtRu/C catalysts for 300 s. Fixed potential: 0.8 V , rotation speed: 600 rpm (the data are derived from the glassy carbon based electrode measurements).

The resistance to poison caused by adsorbed intermediates is another crucial concern for the catalysts from the viewpoint of application. Generally, the ratio of the forward anodic peak current density (I_f) to the reverse anodic peak current density (I_b), I_f/I_b , can be used to describe the tolerance of the catalyst to the accumulation of carbonaceous species. A low I_f/I_b ratio indicates poor oxidation of alcohol to carbon dioxide during the anodic scan, and excessive accumulation of carbonaceous residues on the catalyst surface. A high I_f/I_b ratio shows the converse case. Based on the results in Fig. 4, I_f/I_b are calculated to be 0.868 for Pt-RuCo/C, 0.629 for PtRu/C and 0.605 for Pt/C. This implies the introduction of Ru or Co into the Pt can improve the tolerance to carbonaceous species accumulation.

Chronoamperometric experiments are carried out to observe the stability and possible poisoning of the catalysts under short-time continuous operation. Fig. 5 shows the evaluation of activity of Pt-RuCo/C and PtRu/C electrodes with respect to time at constant potential of 0.8 V (versus RHE). It is clear that the Pt-RuCo/C electrode is more stable than the PtRu/C electrode. Besides the small

particle size and large electrochemical active surface areas, the better performance of the Pt-RuCo/C may be attributed to the coexistence of Ru and Co. Ru can transform CO-like poisoning species on Pt into CO₂, leaving the active sites on Pt for further adsorption and oxidation of ethanol molecules by the bifunctional mechanism and/or a “ligand effect” [21, 22]. Co can improve the ethanol electrooxidation performance in acid solution [23]. Furthermore, the alloying degree of Pt, Ru and Co in the catalyst is an important parameter that can also affect the catalytic performance, which is under investigation in our laboratory

4. CONCLUSIONS

The well dispersed and narrowly distributed Pt-RuCo nanoparticles with low noble metal content supported on Vulcan XC-72 carbon are successfully synthesized by a facile two-step method. The average particle size determined by XRD and TEM is about 3.0 nm. Electrochemical measurements indicate that the catalytic performance of the Pt-RuCo/C catalyst for ethanol electrooxidation is better than that of the Pt/C and PtRu/C catalysts. Consider the relatively low cost of the catalyst, the Pt-RuCo/C is a strong candidate catalyst for ethanol electro-oxidation.

ACKNOWLEDGMENTS

We would like to thank the National Natural Science Foundation of China (Project No. 51001052), the Natural Science Foundation of Guangdong Province (Nos. 10451601501005315 and 10451601501006188) and the Science & Technology project of Huizhou City (2010B020008017) for financially supporting this work.

References

1. W. Zhou, Z. Zhou, S. Song, W. Li, G. Sun, P. Tsiakaras and Q. Xin, *Applied Catalysis B: Environmental*, 46 (2003) 273.
2. S. Rousseau, C. Coutanceau, C. Lamy and J.-M. Léger, *J. Power Sources*, 158 (2006) 18.
3. H.-F. Wang and Z.-P. Liu, *J. Phys. Chem. C*, 111 (2007) 12157.
4. J. Parrondo, R. Santhanam, F. Mijangos, B. Rambabu, *Int. J. Electrochem. Sci.*, 5 (2010) 1342 .
5. A. O. Neto, R. W. R. Verjullo-Silva, M. Linardi and E.V. Spinacé, *Int. J. Electrochem. Sci.*, 4 (2009) 954.
6. S. Tanaka, M. Umeda, H. Ojima, Y. Usui, O. Kimura, I. Uchida, *J. Power Sources*, 152(2005) 34.
7. G. Andreadis and P. Tsiakaras, *Chem. Eng. Sci.*, 61 (2006) 7497.
8. W.J. Zhou, S.Q. Song, W.Z. Li, Z.H. Zhou, G. Q. Sun, Q. Xin, S. Douvartzides and P. Tsiakaras, *J. Power Sources*, 140 (2005) 50.
9. Y.L. Guo, Y.Z. Zheng and M.H. Huang, *Electrochim. Acta*, 53 (2008) 3102.
10. V. P. Santos and G. Tremiliosi-Filho, *J. Electroanal. Chem.*, 554-555 (2003) 395.
11. T. Frelink, W. Visscher, A.P. Cox and J.A.R. van Veen, *Electrochim. Acta*, 40 (1995)1537.
12. Z.-B. Wang,, G.-P. Yin and Y.-G. Lin, *Journal of Power Sources*, 170 (2007) 242.
13. J. Zhu, F.Y. Cheng, and Z.L. Tao, *J. Phys. Chem. C*, 112 (2008) 6337.
14. L.X. Yang, R.G. Allen, K. Scott, P. Christenson and S. Roy, *J. Power Sources*, 137(2004) 257.
15. V. Neburchilov, H.J. Wang and J.J. Zhang, *Electrochem. Commun.*, 9 (2007) 1788.

16. T. Huang, J.L. Liu, R.S. Li, W.B. Cai and A.S. Yu, *Electrochem. Commun.*, 11 (2009) 643.
17. B. Moreno, J.R. Jurado and E. Chinarro, *Catal. Commun.*, 11 (2009) 123.
18. A.B. Kashyout, A. B. A.A. Nassr, L. Giorgi, T. Maiyalagan and B. A. B. Youssef, *Int. J. Electrochem. Sci.*, 6 (2011) 379.
19. R.F. Wang , H. Li, S. Ji, H. Wang and Z.Q. Lei, *Electrochimica Acta*, 55 (2010) 1519.
20. X. Li, W.X. Chen, J. Zhao, W. Xing and Z.D. Xu, *Carbon*, 43 (2005) 2168.
21. T. Iwasita, *Electrochim. Acta*, 47 (2002) 3663.
22. T. Frelink, W. Visscher and J.A.R. Van Veen, *Surf. Sci.*, 335(1995)353.
23. T. Page, R. Johnson, J. Hormes, S. Noding and B. Rambabu, *J. Electroanal. Chem.*, 485 (2000) 34.